

City \mathcal{X} : Controllable Procedural Content Generation for Unbounded 3D Cities

Shougao Zhang^{2*} Mengqi Zhou^{1*} Yuxi Wang^{5*} Chuanchen Luo⁴ Rongyu Wang¹
 Yiwei Li¹ Zhaoxiang Zhang^{1,3,5†} Junran Peng^{1,3,6†}

¹University of Chinese Academy of Sciences, ²China University of Geosciences (Beijing)

³Institute of Automation, Chinese Academy of Sciences (CASIA), ⁴Shandong University

⁵Centre for Artificial Intelligence and Robotics, (HKISI-CAS), ⁶University of Science and Technology Beijing

zhangshougao@email.cugb.edu.cn, jrpeng4ever@126.com, zhoulm2022@ia.ac.cn

yuxi.wang93@gmail.com, chuanchen.luo@sdu.edu.cn, zhaoxiang.zhang@ia.ac.cn

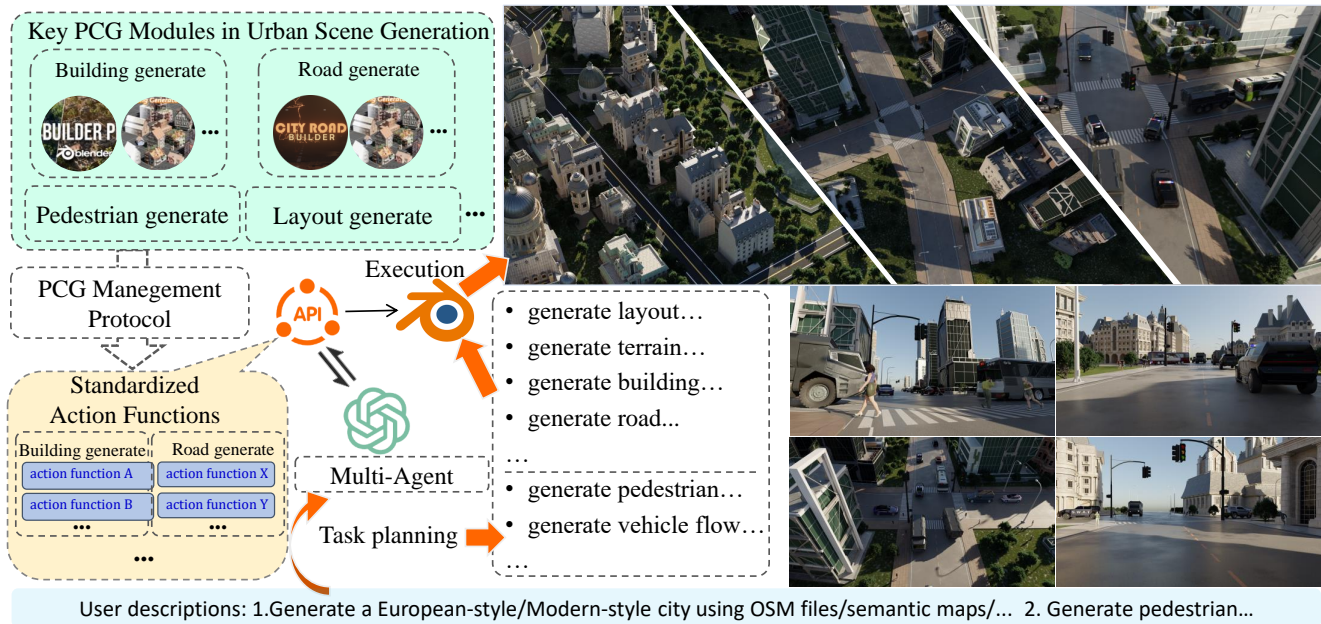


Figure 1. The proposed City \mathcal{X} can generate high-quality, controllable, and editable large-scale urban scenes based on user descriptions and multimodal inputs (OSM files, semantic maps, satellite images). The generated scenes allow for the integration of dynamic elements, such as pedestrians and traffic, ensuring a fully interactive and adaptable environment.

Abstract

Urban areas, as the primary human habitat in modern civilization, accommodate a broad spectrum of social activities. With the surge of embodied intelligence, recent years have witnessed an increasing presence of physical agents in urban areas, such as autonomous vehicles and delivery robots. As a result, practitioners significantly value crafting authentic, simulation-ready 3D cities to facilitate the training and verification of such agents. However, this task is quite challenging. Current generative methods fall short in either diversity, controllability, or fidelity. In this work, we resort to the procedural content generation (PCG) technique for high-fidelity generation. It assembles superior assets according to empirical rules, ultimately leading to industrial-grade outcomes. To ensure diverse and

self-contained creation, we design a management protocol to accommodate extensive PCG plugins with distinct functions and interfaces. Based on this unified PCG library, we develop a multi-agent framework to transform multi-modal instructions, including OSM, semantic maps, and satellite images, into executable programs. The programs coordinate relevant plugins to construct the 3D city consistent with the control condition. A visual feedback scheme is introduced to further refine the initial outcomes. Our method, named City \mathcal{X} demonstrates its superiority in creating diverse, controllable, and realistic 3D urban scenes. The synthetic scenes can be seamlessly deployed as a real-time simulator and an infinite data generator for embodied intelligence research. Our project page: <https://cityx-lab.github.io/>.

1. Introduction

With the development of civilization, cities have become the primary human habitat, supporting a wide range of social activities. It is characterized by a complex layout, diverse buildings, interlaced roads, and esthetic streetscape. Due to rapid advancements in robotics and embodied AI, there has been a notable increase in the presence of physical agents in urban areas, including autonomous taxis, unmanned aerial vehicles (UAVs), and mobile robots designed for delivery, cleaning, and service. These intelligent agents not only enhance the convenience of daily life for residents but also boost the economic efficiency of society. By providing a secure and interactive environment for training and verification, urban simulator greatly facilitates the development of such agents. As a critical component of the urban simulator, 3D city creation has attracted significant attention from both industry and academy. The simulator has demands a high degree of diversity, controllability, and fidelity in synthetic urban scenes. These properties are necessary prerequisite for robots to generalize to real-world scenarios. Such a task is particularly challenging. A senior designer generally spend a few days crafting a desirable city scene from scratch.

Recently, some methods [8, 27, 47] have emerged to automate the creation of 3D urban scenes. A mainstream practice is to lift 2D generative representation to 3D space. For instance, InfiniCity [27] and CityDreamer [47] condition neural radiance field on the bird’s-eye-view layout feature map. Qualitative results show that these methods suffer from fuzzy appearance or irregular geometry. Moreover, the implicit neural scene representation they used is not compatible with existing simulation engines. These drawbacks prevent them from practical application. Realizing the significant gap between the strict demands and the performance of neural methods, researchers have attempted to borrow inspiration from mature industrial pipelines recently. Procedural content generation (PCG), as a key technique in video game development, is frequently employed for the rapid creation of exquisite scenes. Each PCG plugin specializes in creating a specific category. It assembles desired assets algorithmically based on the empirical rules which are derived by profound analysis in the patterns of instances belonging to this category. The PCG synthetic assets fully meet the industrial requirements and are seamlessly compatible with simulation engines. 3D-GPT [39], Scenecraft [18], and SceneX [53] are three pioneer methods that resort to the PCG paradigm for scene generation. They leverage the powerful planning capability of large language models (LLMs) to orchestrate PCG programs according to text instructions. Despite their favorable performance against those neural methods, these methods are initially designed for the creation of general scenes and have not been tailored for urban scenes. They only support the control of

textual instructions which is too coarse for the 3D urban creation. While in the industrial pipeline, the designers need to arrange relevant assets, such as buildings, streets, and bridges, according to the layout constraints which are generally defined by OpenStreetMap or semantic maps. Moreover, current solutions are deficient in adaptability and scalability. They lack the ability to coordinate PCG plugins with distinct functions and incompatible interfaces, which in turn impedes the creation of self-contained urban scenes.

In this paper, we introduce an efficient and productive pipeline, named City \mathcal{X} , for the controllable creation of diverse and high-fidelity 3D cities. To tackle challenges in the integration of various plugins, we first develop a management protocol to reformat the interface of different assets. The protocol primarily comprises two parts: (i) a dynamic API conversion interface, enabling free and flexible integration of plugins with different functions; (ii) structured encapsulation, formatting the plugins for subsequent calling. The proposed protocol shows the potential to build an ecosystem for the community, which is crucial for unifying various PCG plugins for the integral creation of complex scenes. Based on this unified protocol, we design a LLM multi-agent framework to automate the orchestration of PCG assets. The framework accepts text descriptions, XML-formatted OSM data, semantic maps, and satellite images as control instructions. The LLM agents perform task planning, plan validation, and action execution sequentially to transform instructions into executable Blender programs. Afterward, Blender interprets the program and renders the scene. A visual language model (VLM) is then introduced to inspect the creation from rendering and offer feedback to refine the initial results further.

Our synthetic 3D cities excel in controllability, diversity, and fidelity. For completeness, we have employed another multi-agent framework to incorporate dynamic elements, such as vehicles and pedestrians, into the synthetic scenes. These dynamic elements navigate and move within their designated feasible areas. Both static and dynamic assets in the scene are interactive, which is essential for tasks involving grasping, manipulation, and active obstacle avoidance. Overall, our synthesized scenes are well-suited to serve as the foundational environment for the simulator.

The contributions of this paper are summarized as follows:

- We propose City \mathcal{X} , an effective and efficient pipeline to create diverse, controllable, and realistic 3D city scenes. Our synthetic scenes are ready for the simulation of embodied AI, facilitating the training and deployment of physical agents.
- We design a management protocol to enable the unified calling of PCG plugins with distinct interfaces, laying the foundation for further extension.
- We develop an LLM-based multi-agent framework to

translate multi-modal instructions into executable blender programs. It coordinates diverse PCG plugins to create harmonized scenes consistent with control conditions.

2. Related Works

Generating a 3D urban scene is a complex task involving multiple modules, such as accurately generating a reasonable layout and then constructing appropriate instances on the layout. Additionally, applying Multi-Agent systems to complex tasks like 3D urban scene generation presents significant challenges. In this section, we will discuss works related to these aspects.

Agent Systems Based on LLMs. When researching agent systems based on Large Language Models (LLMs), the focus lies on effectively integrating and applying these models to execute complex tasks. Existing relevant work encompasses various aspects, including task management, role-playing, dialogue patterns, and tool integration. For example, [19] utilizes the expansive domain knowledge of LLMs on the internet and their emerging zero-shot planning capabilities to execute intricate task planning and reasoning. [15] investigates the application of LLMs in scenarios involving multi-agent coordination, covering a range of diverse task objectives. [51] presents a modular framework that employs structured dialogue through prompts among multiple large pretrained models. Moreover, specialized LLMs for particular applications have been explored, such as HuggingGPT [38] for vision perception tasks, VisualChatGPT [45] for multi-modality understanding, Voyager [43] and [54], SheetCopilot [23] for office software, and Codex [4] for Python code generation. Furthermore, AutoGPT[7] demonstrates the ability to autonomously complete tasks by enhancing AI models, but it is a single-agent system and does not support multi-agent collaboration. In contrast, BabyAGI[30] uses multiple agents to manage and complete tasks, with each agent responsible for different task modules such as creating new tasks, prioritizing the task list, and completing tasks. Multi-agent debate research includes works[26][10] indicating that debates among multiple LLM instances can improve reasoning and factuality, but these methods typically lack the flexibility of tool and human involvement. AutoGen[46], as a general infrastructure, supports dynamic dialogue modes and a broader range of applications, demonstrating potential in advancing this field.

3D Urban Scene Generation. Scene-level content generation presents a challenging task, unlike the impressive 2D generative models primarily targeting single categories or common objects, due to the high diversity of scenes. Semantic image synthesis, as exemplified by [11, 17, 29, 34], has shown promising results in generating scene-level content in the wild by conditioning on pixel-wise dense correspondence, such as semantic segmentation maps or depth

maps. Recent works such as [2, 6, 27] have realized infinite-scale 3D consistent scenes through unbounded layout extrapolation. Additionally, in-depth research has been conducted on using procedural content generation (PCG) techniques to generate natural scenes [13, 52] and urban scenes [28, 40, 42, 50]. For example, PMC [33] proposed a procedural method based on 2D ocean or city boundaries to generate cities. It employs mathematical algorithms to generate blocks and streets and utilizes subsequent techniques to generate the geometric shapes of buildings. While traditional computer graphics methods can generate high-quality 3D data, all parameters must be predefined during the procedural generation process. Since the generated 3D data is subject to rule limitations and exhibits a certain degree of deviation from the real world, this significantly constrains its flexibility and practical utility.

3. Methods

The overall objective is to generate high-quality, controllable, and editable interactive large-scale city scenes in multiple stages based on natural language instructions and multimodal inputs. To achieve this goal, we propose the City \mathcal{X} framework, where we use procedural generation(PCG) to construct the entire scene and leverage our designed multi-agent system to enable the LLM to parse parameters and act as an agent based on natural language instructions. In Sec 3.1, we described the relevant PCG modules we have collected and created based on the requirements of the urban scene generation task. In Sec 3.2, we describe the PCG management protocol we designed to standardize and manage the PCG modules, ensuring their compatibility and scalability. In Sec 3.3, we present our multi-agent system, optimized with visual feedback, which supports the flexible, fast, and accurate construction of urban scenes based on language descriptions and multimodal inputs. In Sec 3.4, we showcase the diverse, high-quality datasets generated through this process, including various formats.

3.1. Key PCG Modules in Urban Scene Generation

To enhance the realism of the generated urban scenes, we categorize the scene elements into roads, buildings, greenery, pedestrians, traffic flow, and water bodies. Among these, roads, buildings, pedestrians, and traffic flow are of particular importance, warranting dedicated PCG modules for each. To support these modules, we have meticulously curated and, in some cases, crafted specialized PCGs for comprehensive integration into the urban environment.

Building Generators. We offer various PCG methods for building generation, such as using L-systems[36] to simulate the basic structure of buildings, akin to the growth process of plants. Through recursive algorithms starting from simple rules, complex architectural forms are progressively generated. Noise functions, such as Perlin noise[35], are

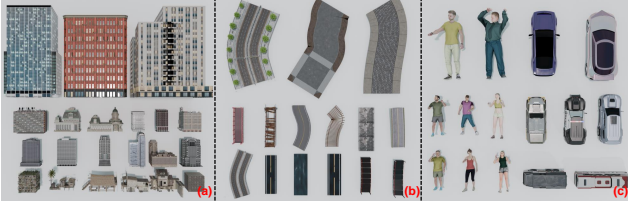


Figure 2. Presentation of PCG modules involved in urban scene generation: building generation PCG effects (a), road generation spline-based PCG effects (b), and dynamic pedestrian and traffic flow generation PCG effects (c).

employed to introduce randomness and variation, preventing the buildings from appearing overly regular or artificial. Fig. 2.(a) illustrates a series of buildings generated using these PCGs. In addition, we have curated and annotated high-quality, artistically crafted building models, recording information such as the building’s footprint and style. For retrieval, we utilize a pre-trained CLIP[37] model, integrating the matching models into the urban scene. Due to space constraints, further details can be found in the appendix.

Roads Generators. We provide various road generators (Fig. 2.(b)) capable of creating common types of roads such as asphalt roads, highways, and secondary roads. These generators support control over parameters such as road width, structure, and style. Roads can be generated based on curves, and some PCGs also generate road materials based on the road’s mesh.

Pedestrian & Vehicle Flow Generators. For pedestrian and traffic flow generation, we also provide relevant PCG modules (Fig. 2.(c)), allowing for additions based on path planning and coordinate inputs. Detailed interactions and input formats are available in the appendix.

3.2. PCG Management Protocol

Recently, existing works 3D-GPT [39], Scenecraft [18] and SceneX [53] have demonstrated the potential of using large language models (LLMs) to orchestrate PCG programs for general scene generation. While these methods have shown promising performance, the quality of the generated scenes often depends heavily on the quality and diversity of the collected PCG assets. However, integrating diverse plugins from various sources is a significant challenge due to the heterogeneity in their interfaces, formats, and functional capabilities. In Sec 3.1, we encountered issues with data format incompatibility among the PCGs we collected. Therefore, we propose a universal PCG management protocol that seamlessly integrates infinite plugin assets to break down the asset barriers in LLM-driven procedural scene generation. The proposed method includes three aspects: *Dynamic API Conversion Interface* and *Structured Encapsulation*.

Dynamic API Conversion Interface. Like HuggingGPT

[38] that integrates external algorithm API with LLMs, the motivation of our Dynamic API Conversion Interface is to provide a universal conversion method that transforms PCG plugins into a format callable by LLM agents. It can empower the LLMs to orchestrate and execute procedural scene generation tasks across a wide range of assets. During the PCG integration process, when a format conversion is needed, the corresponding interface can be automatically invoked for the conversion. For instance, we can convert the curve of the road in this step to a plane, allowing the downstream PCG to continue the subsequent tasks. This dynamic API conversion interface serves as a bridge between different APIs, providing communication interfaces for various API formats. By dynamically adjusting these interfaces, we can achieve the flexible combination of different PCGs. We provide detailed conversion examples and an analysis of interface format types in the appendix.

Structured Encapsulation. Since LLM cannot directly use PCG through Blender, it is necessary to encapsulate PCG into action functions that are executable by LLM. Additionally, we need to parameterize each PCG so that LLM can plan tasks more accurately based on the functional boundaries of the PCG. Moreover, encapsulating PCG into action functions presents significant technical barriers for beginners, particularly in terms of coding knowledge and 3D modeling expertise. To help beginners quickly and easily create their own action functions, we propose a method of structured encapsulation. For each PCG, the encapsulation, denoted as Encapsulation S , follows a similar structure defined as $S_i(C_i, D_i, I_i, L_i, R_i)$, where i distinguishes the i -th action function. The components of the protocol are defined as follows:

- **Classname** The name of the action function, used for indexing the action function.
- **Description** A detailed objective description of an action function.
- **Input** A detailed objective description of the input to the action function.
- **Limitation** An objective description of the functional constraints of the action function.
- **Run** Function name used to execute the action function and return the result.

We provide users with a straightforward encapsulation document. By acquainting themselves with the process of extracting API information from Blender, users can seamlessly follow the document’s instructions to encapsulate their own functional actions.

3.3. Multi-Agent Framework

Fig. 3 illustrates the overall generation workflow of City \mathcal{X} , with its core components comprising the PCG management protocol module and the multi-agent module. Due to the need for efficient multi-stage interactive generation, such as

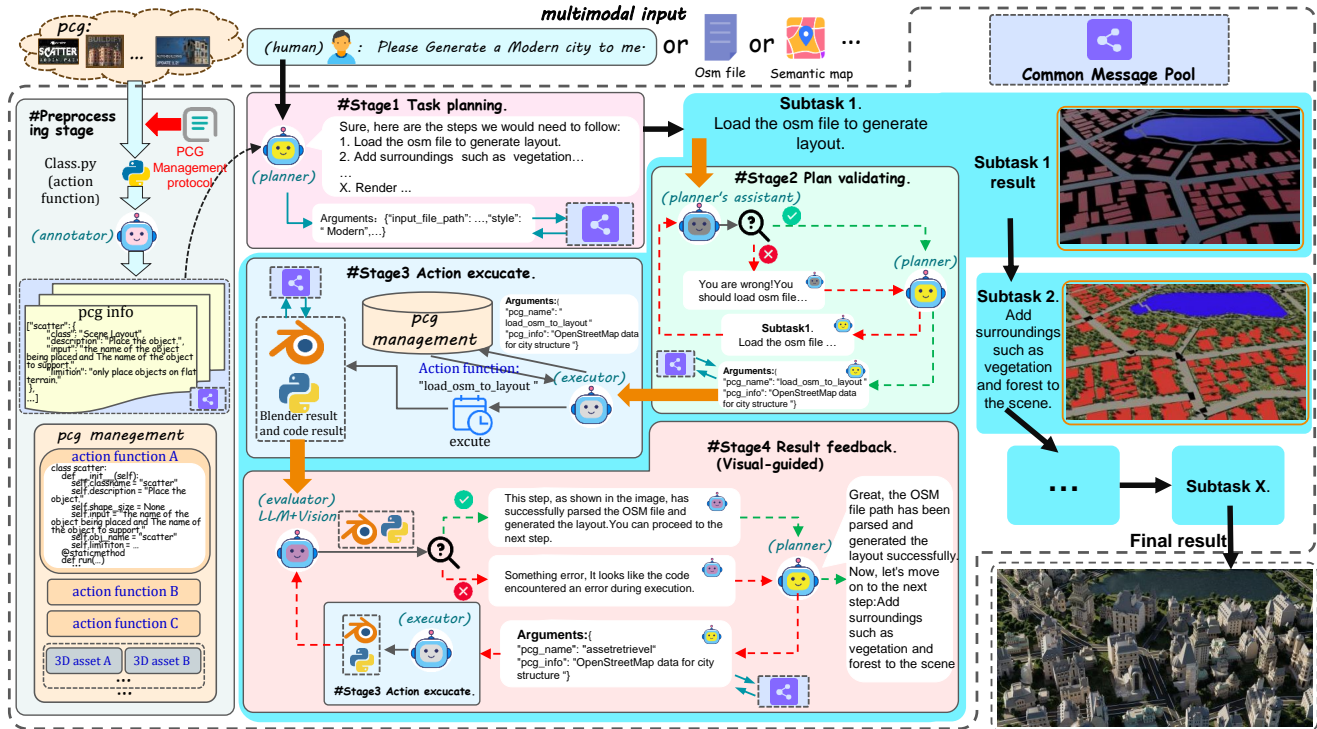


Figure 3. Multi-agent Workflow: Detailed demonstration of collaboration and communication across various stages.

the blueprint for layout planning, the geometry node for asset scatter, and numerous parameters for asset placement, color, size, and height, this renders a naive LLM framework inadequate for handling Blender’s complex and diverse action. This framework mainly consists of four agents: annotator, planner, executor, and evaluator. The annotator labels all actions with multiple tags and stores the annotated action information in the common message pool. The planner formulates the overall task pipeline using user-provided textual information and determines the action required for different sub-tasks. The executor manages all action functions and uses the annotated action functions to process sub-tasks of PCG or asset manipulation in Blender. The evaluator assesses the correctness of the current sub-task by obtaining scene information from Blender, such as object location and rendered images.

Multimodal Input through Multi-Agent Framework.

Unlike simple LLM frameworks, our Multi-Agent Framework can find feasible solutions through multiple rounds of interaction and visual feedback, meaning that with only a few plugins, the target task can be accomplished, avoiding the burden to reinvent the wheel. This also simplifies city generation through multimodal inputs. For example, when we import a semantic map into Blender, it is stored as a point cloud containing semantic information, but we only have face-based building generation actions. At this point, the Multi-Agent Framework will find a tool to convert vertices into faces, complete the conversion, and then use face-

based building generation actions to accomplish the task.

Annotator Agent. For large-scale city generation tasks, a substantial number of action functions are required. Therefore, effectively managing these action functions is crucial. To ensure each agent can efficiently access all action of different hierarchies, we use the Annotator to label them. More details of the annotations are provided in the appendix, along with relevant examples.

Planner Agent. We consider PCG-based city scene generation as an open-loop planning task with flexible steps. Specifically: (i) Termination of the city scene generation task depends on meeting the user’s requirements; (ii) City scene generation tasks are a series of sequentially arranged action functions, where the order of these actions significantly impacts the final outcome. To address these challenges, we propose a dynamic planner. At the beginning of the task, the planner formulates a rough workflow as a reference. During the execution of specific sub-tasks, the planner plans the next action based on the current sub-task goals and the workflow, until the user’s requirements are met.

When the planner directly receives user input, it needs to translate the user’s intent into a series of referable executable actions with additional explanations, which will be stored in the common message pool. To achieve this, we prompt the planner to produce a preliminary action plan, serving as the workflow. Specifically, we utilize the labeled information L from the common message pool, the user in-

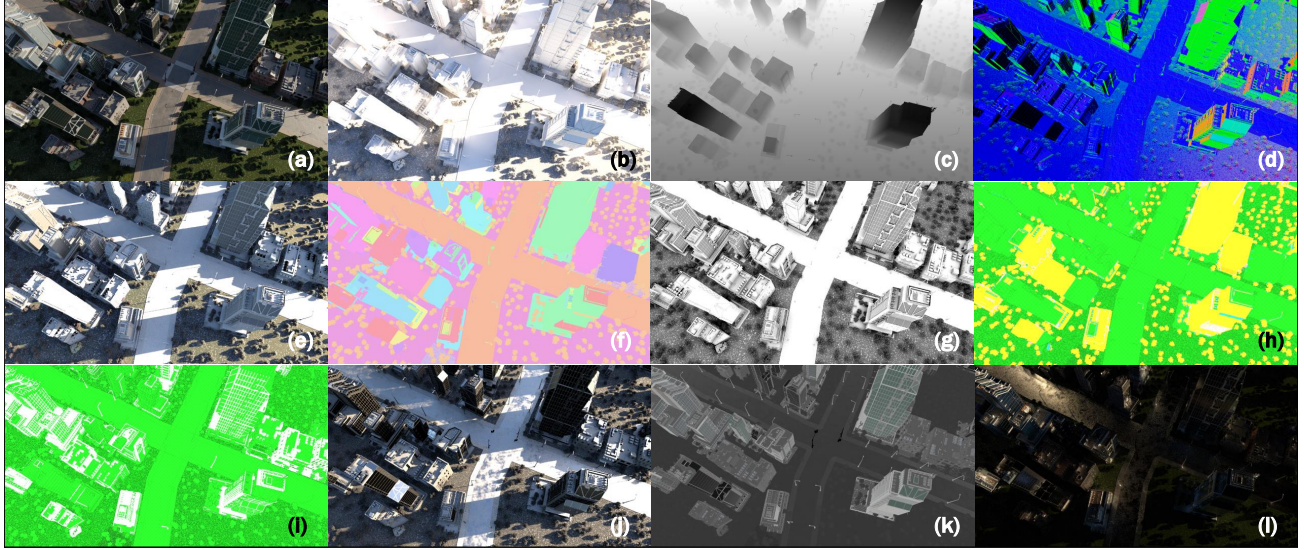


Figure 4. For each image (a), we have a high-resolution mesh (b), which readily yields Depth (c), Surface Normals (d), Diffuse Map (e), Instance Segmentation masks (f), Ambient Occlusion (g), Cryptomatte Object/Material Mask (h/i), and Glossy Direct/Color/Indirect (j/k/l). We used a 1920×1080 resolution with 10,000 random samples per pixel, a standard setting in Blender that effectively eliminates sampling noise, resulting in a high-quality final image.

put I , and the planner’s guidance document D as inputs, allowing the planner to generate an ordered workflow W . This process is formalized as follows:

$$W \leftarrow \text{Planner}(L, I, D) \quad (1)$$

During the execution of the t -th sub-task, the planner needs to formulate actions required for the $(t + 1)$ -th sub-task. To ensure the accuracy and coherence of actions, the planner refers to the workflow. Specifically, based on the ordered workflow W , sub-task input I , the labeled information L from the common message pool, and the planner’s guidance document D , the planner infers the next action A_{t+1} , where A_{t+1} stands for the action of the $(t + 1)$ -th sub-task.

$$A_{t+1} \leftarrow \text{Planner}(L, I, D, W). \quad (2)$$

Executor Agent. To achieve Interactive Workflow in Blender, we deploy the Executor within the Blender environment. All agents send action execution commands to the Executor through a local backend server. As mentioned in Sec 3.1, we transform PCG plug-ins into executable action functions using structured encapsulation. This allows the Executor to initialize all actions flexibly. To enable agents to precisely control actions, each action function is structurally recorded in JSON format. For example, the `scale_object` action function is documented as follows:

```
scale_object_doc = {name: scale_object,
  description: Scale an object,
  parameters: {scale_factor: {type: tuple,
    description: scale factor},
    scaled_obj_name: {type: str, description:
      scaled object name}}}
```

During the execution of the t -th sub-task, the Executor uses the action document D and the sub-task input I to generate the action arguments $Arguments$. The action A_t is then executed in Blender based on the arguments. Here, A_{t+1} represents the action for the $(t + 1)$ -th sub-task, S_{t+1} represents the Blender state for the $(t + 1)$ -th sub-task, and S_t represents the Blender state for the t -th sub-task.

$$\begin{aligned} Arguments &\leftarrow \text{Executor}(I, D), \\ S_{t+1} &\leftarrow \text{Blender}(S_t, A_t, Arguments) \end{aligned} \quad (3)$$

Evaluator Agent. To address the limitations of textual feedback in urban scene generation tasks, we designed an Evaluator with visual feedback based on GPT-4V[31]. Specifically, we first render the generated scene as an image. Then, we provide both the image and the current sub-task text input to the Evaluator, guiding it with prompts to assess whether the scene’s geometry and materials match the sub-task expectations. If the Evaluator determines that the rendered image is consistent with the sub-task text input in terms of geometry and materials, the evaluation ends. However, if the Evaluator identifies errors, it can pass this information to the Planner for improvements. This process is formalized as follows:

$$R \leftarrow \text{Evaluator}(\text{GPT-4V}(img, I, D)), \quad (4)$$

where R stands for the Evaluator result, img stands for the rendered image, I stands for the sub-task input, and D stands for the Evaluator’s guidance document.

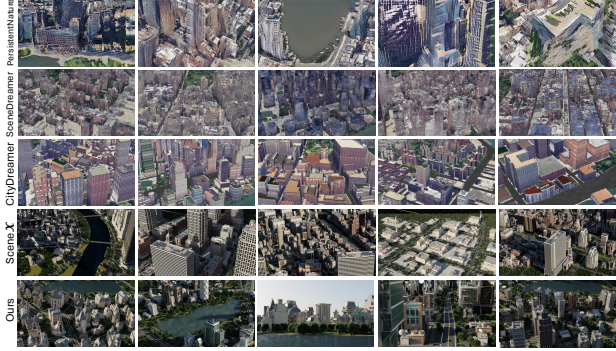


Figure 5. Comparative results on city generation. Issues with unreasonable geometry are observed in previous works, while our method performs well in generating realistic large-scale city scenes.

3.4. Urban Scene Dataset Synthetic

Based on the scenes we have built, we can generate an unlimited number of high-quality city scene datasets, which are rendered using Blender’s physically-based path tracing renderer, Cycles, as shown in Fig. 4. The scenes that can be generated are infinite, and thus the dataset is also unlimited. Previous related datasets often faced issues such as high production costs or lower quality. However, our implementation is highly efficient and low-cost. We compare the advantages of our dataset with other urban scene datasets in the appendix and present more details about the datasets. We anticipate that users will be able to easily extend our codebase to generate various city scene datasets, meeting the needs of applications in related fields.

4. Experiments

The goals of our experiments are threefold: (i) to verify the capability of City \mathcal{X} for generating highly realistic large-scale city with different modes of input; (ii) to prove that the Muti-Agent framework and pcg protocol we designed are effective; (iii) to compare different LLMs on the proposed benchmark.

4.1. Benchmark Protocol

Dataset. To evaluate the effectiveness of the proposed City \mathcal{X} , we collect 50 city Semantic Maps, 50 city Height Fields, and 50 city OSM files in XML format. We also collect 50 sets of descriptions about city styles and weather. Then, we feed them to our City \mathcal{X} to generate corresponding city models, which are used to perform quantitative and qualitative comparisons.

Models. When generating and editing the 3D scenes, we adopt the leading GPT-4 as the large language model with its public API keys. To ensure stable output from the LLM, we set both the decoding temperature and the seed to 0.

Metrics: We use Executability Rate (ER@1) and Success

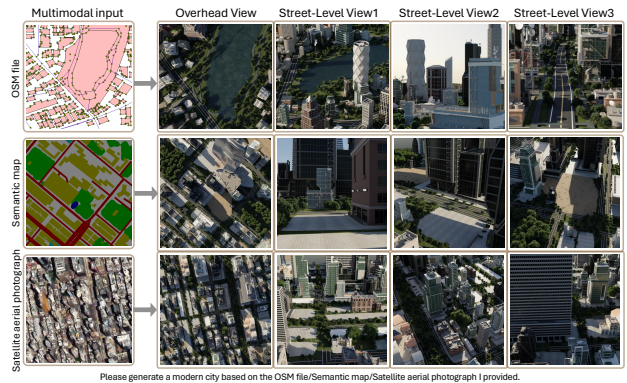


Figure 6. Urban scene generation with multimodal inputs, where we present an overhead view aligned with the multimodal input perspective, along with three street-level views.

Table 1. Comparing the performance of different language models in city generation. The aesthetic score represents the intuitive aesthetic rating, and the rationality score is the logical coherence rating. Where "AS" represents the average score (from 30 volunteers), and "AES" represents the average expert score (from 5 graphics experts).

Model	AS		AES	
	aesthetic score	rationality score	aesthetic score	rationality score
CityDream[47]	2.80	3.05	2.65	3.40
PersistentNature[2]	1.30	1.40	1.55	1.35
SceneDreamer[6]	1.30	1.63	1.30	1.35
Scene \mathcal{X} [53]	3.73	3.63	3.50	3.45
City \mathcal{X} (Ours)	4.30	4.35	4.15	4.30

Rate (SR@1) to evaluate the capabilities of LLMs on our City \mathcal{X} . The former measures the proportion of proposed actions that can be executed, and the latter is used to evaluate action correctness [5]. Additionally, we use a unified evaluation standard as a reference. We categorize the aesthetics of city scenes into five levels: Poor (1 points)/Below Average (2 points)/Average (3 points)/Good (4 points)/Excellent (5 points).

4.2. Main Result

Urban Scene Generation with Multimodal Inputs. We first show the ability of City \mathcal{X} to generate large-scale urban scenes, as depicted in Fig. 6. The results show that City \mathcal{X} is capable of generating highly realistic urban scenes using multimodal data inputs, including OSM data, semantic maps, and satellite images, demonstrating its effectiveness and flexibility in urban scene generation.

We also compare our method with other city generation approaches, as shown in Fig. 5. The results indicate that PersistentNature[2] and InfiniCity[27] have severe deformation issues throughout the entire scene. While SceneDreamer[6] and CityDreamer[47] demonstrate improved structural consistency, their building quality remains relatively low. While Scene \mathcal{X} [53] achieves high quality, it encounters issues with overlapping assets and a high dupli-

cation rate of buildings. In contrast, the city generated by City \mathcal{X} demonstrates a regular geometric structure and high quality, which is devoid of overlapping buildings and exhibits minimal repetition.

Aesthetic Evaluation. To better assess the quality of cities generated by City \mathcal{X} , we collect results from various related works on urban generation and invite 30 volunteers and 5 experts in 3D modeling to evaluate these works aesthetically. To ensure fairness, we anonymize all results. As shown in Tab. 1, the cities generated by City \mathcal{X} attain a "Good" level in aesthetic scoring, a distinction not achieved by other works, demonstrating its highly realistic capabilities in city generation.

Specific Refinement Editing. City \mathcal{X} supports specific refinement editing for scene customization, involving asset manipulation, weather adjustment, and style modification. We conduct relevant experiments, as depicted in Fig. 7. Based on the results, it's clear that City \mathcal{X} performs well in accurately controlling urban scenes to meet input requirements consistently.

Table 2. Ablation Study Results for Different Components of the Protocol.

Description.	Input	Limitation	ER@1	SR@1
		✓	36.00	41.67
	✓	✓	37.00	51.35
✓			44.00	56.82
✓	✓		69.00	60.87
✓		✓	73.00	61.64
✓	✓	✓	94.00	82.98

Table 3. Comparing the performance of different language models in city generation.

Model	ER@1	SR@1
Llama2-7B[41]	27.00	59.26
Mistral[20]	78.00	61.54
Gemma-2B[14]	9.00	33.33
Gemma-7B[14]	39.00	69.23
GPT-3.5-turbo[1]	72.00	75.00
GPT-4[32]	91.00	81.32

4.3. Ablation Study of PCG Protocol.

Analysis of Different Components. To assess the impact of each component of the structured encapsulation on the overall system, we conduct ablation experiments on individual parts of the structured encapsulation, as shown in Tab. 2. The table demonstrates that when encapsulating PCG, adding Description, Input, and Limitation all boost ER@1 and SR@1. Notably, including Description leads to the highest increase, with SR@1 rising by 57.00% and

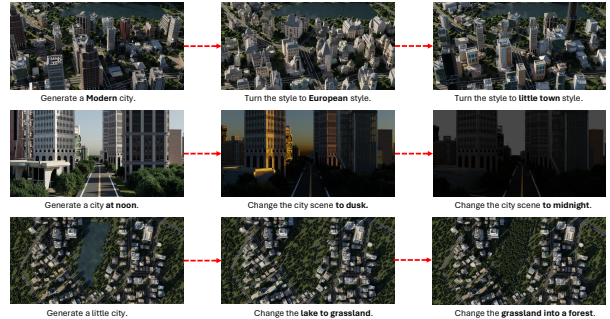


Figure 7. Performance of City \mathcal{X} in scene customization and refinement editing

ER@1 by 31.63%, significantly enhancing the system's Executability Rate and Success Rate. After adding Input, SR@1 and ER@1 increase by up to 21.34% and 25.00%, respectively. Similarly, with the inclusion of Limitation, SR@1 and ER@1 see maximum increases of 22.11% and 25.00%. This suggests that incorporating Input and Limitation can improve the system's Executability Rate and Success Rate.

Comparing Agent Frameworks with Different LLMs To evaluate the effects of different large language model variants on multi-agent frameworks, we assessed the system's ER@1 and SR@1 using various LLM versions. As not all open-source models have visual perception capabilities, we used GPT-4-Vision-Preview uniformly for visual feedback. To maintain experimental stability, the temperature and seed for all LLMs were set to 0. The experiment utilized 50 description sets from Section 4.1 dataset. Results are shown in Tab. 3. GPT-4 achieves the highest scores in both ER@1 and SR@1, with scores of 91.00% and 89.01%, respectively. Mistral ranks second in ER@1, with a score of 78.00%, while GPT-3.5-turbo and Gemma-7B rank second and third in SR@1, with scores of 75.00% and 69.23%, respectively. It is evident that Mistral and Gemma-7B, two open-source large language models, perform comparably to GPT-3.5-turbo but still fall short of GPT-4's performance.

5. Conclusion

This paper presents a streamlined and productive pipeline for controllable 3D urban scene generation. Rather than creating scenes from scratch using neural generative models, we resort to the procedural generation paradigm. We design a management protocol to enable flexible integration and free calling. A multi-agent framework powered by LLMs is introduced to automate the creation process according to multi-modal instructions, such as OSM. Our generated scenes are interactable and superior in controllability, diversity, and fidelity, making them well-suited as base environments for simulators. Our method has the potential to significantly advance the field of embodied intelligence.

Appendix

A. Implementation Details

A.1. Key PCG Modules

We roughly divide the city scene generation into the following stages:

$$S = \{S_{\text{layout}}, S_{\text{terrain}}, S_{\text{building}}, S_{\text{road}}, S_{\text{nature}}, S_{\text{background}}\}, \quad (5)$$

where S_{layout} represents layout generation, S_{terrain} represents terrain generation, S_{building} represents building generation, S_{road} represents road generation, S_{nature} represents nature elements generation (including vegetation, rivers, lakes, etc.), and $S_{\text{background}}$ represents background generation (e.g., weather and sunlight).

The dependency relationships between stages can be expressed as a directed graph:

$$G = (V, E), \quad (6)$$

where $V = S$ is the set of stages, and E is the set of dependencies. For example, $(S_{\text{layout}}, S_{\text{building}}) \in E$ indicates that building generation depends on layout generation. However, certain stages, such as S_{building} and S_{road} , do not require a specific order.

Each stage S_i comprises a set of PCG (Procedural Content Generation) modules:

$$S_i = \{M_{i,1}, M_{i,2}, \dots, M_{i,k_i}\}, \quad (7)$$

where $M_{i,j}$ is the j -th module in the i -th stage, and k_i represents the total number of modules in that stage.

Given specific requirements R , the system selects PCG modules that satisfy the requirements from each stage:

$$M_{\text{selected}} = \bigcup_{i \in \{1,2,\dots,n\}} \{M_{i,j} \mid M_{i,j} \text{ satisfies } R\}. \quad (8)$$

The generation process for different cases can be represented as specific sequences of selected modules:

$$F_{\text{case}} = [M_{i_1,j_1}, M_{i_2,j_2}, \dots, M_{i_m,j_m}], \quad (9)$$

where F_{case} denotes the generation pipeline for a particular case, and the sequence of modules is determined based on the requirements or task logic.

Fig. 8 illustrates the task phases and PCG module counts in the overall city generation and editing process we collected. During execution, specific requirements guide the selection and execution of tasks by a multi-agent system. Fig. 9 presents an example case, demonstrating the generation process and the selected PCG modules involved.

A.2. Dynamic Element Generation and Interactive Editing

After the successful generation of the urban scene, we provide various implementations for interactive editing (e.g., editing specific elements in the scene) and the generation of dynamic elements (e.g., pedestrians, vehicle traffic). The entire workflow can be divided into two main parts: interactive input and specific execution. Interactive input focuses primarily on the extraction and transformation of information, such as determining the location or path for generating dynamic elements. For example, when we want to add a running character at a specific location in the scene, we can input this information by describing the path location or directly drawing a curve in the scene. This information is then processed through the corresponding PCG module, generating the corresponding instance (e.g., a curve object) in the Blender scene. After converting the path into a curve in the scene, the additional parameters related to the running character (e.g., speed, posture, clothing) are used to generate and insert the "running character" into the scene using the corresponding PCG module. The following pseudocode Algorithm .1 shows the specific implementation of adding a pedestrian. Similarly, the generation of vehicle traffic and other interactive editing processes also follow the pattern of first transforming input and then using the corresponding PCG module for execution. Fig. 8 shows the number of PCGs involved in adding dynamic elements, as well as the number of PCGs supporting interactive editing functionalities.

A.3. Details of PCG Management Protocol

Dynamic API Conversion Interface. In Sec 3.2, we discussed that the primary reason for the incompatibility among PCG modules lies in the difficulty of standardizing input and output data formats during the workflow transitions between different modules. Specifically, we first catalog all the possible input and output formats we have currently collected for the PCGs, as shown on the left side of Tab. 4. These data formats represent the proportion of input and output formats in PCG. Based on this, we define a comprehensive and self-consistent dynamic API conversion interface, as shown on the right side of the Tab. 4. During the PCG integration process, when a format conversion is needed, the corresponding interface can be automatically invoked for the conversion. For instance, we can convert the curve of the road in this step to a plane, allowing the downstream PCG to continue the subsequent tasks. This dynamic API conversion interface serves as a bridge between different APIs, providing communication interfaces for various API formats. By dynamically adjusting these interfaces, we can achieve the flexible combination of different PCGs.

Structured Encapsulation. A crucial component of the protocol is structured encapsulation, for which we have de-

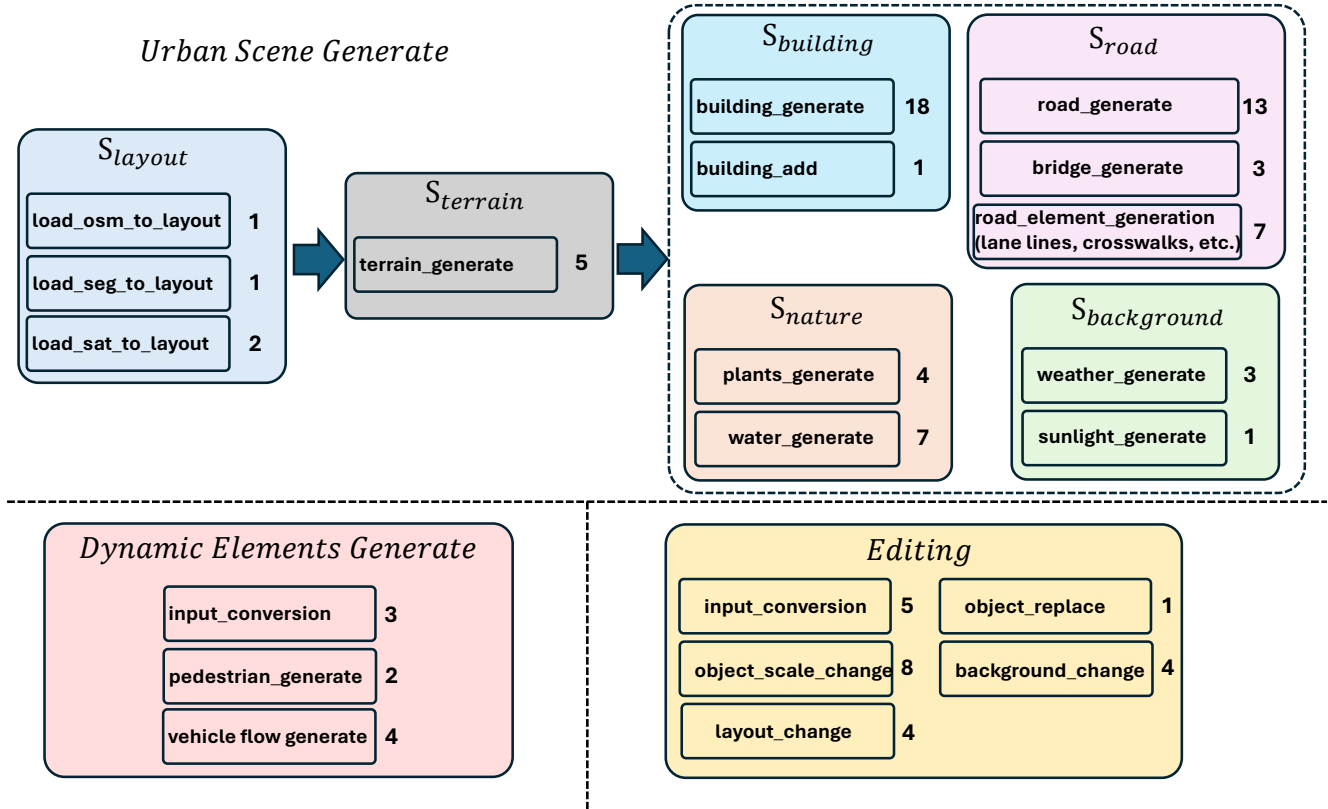


Figure 8. Task phases and PCG module counts in the overall city generation and editing process, with multi-agent system guidance for task selection and execution.

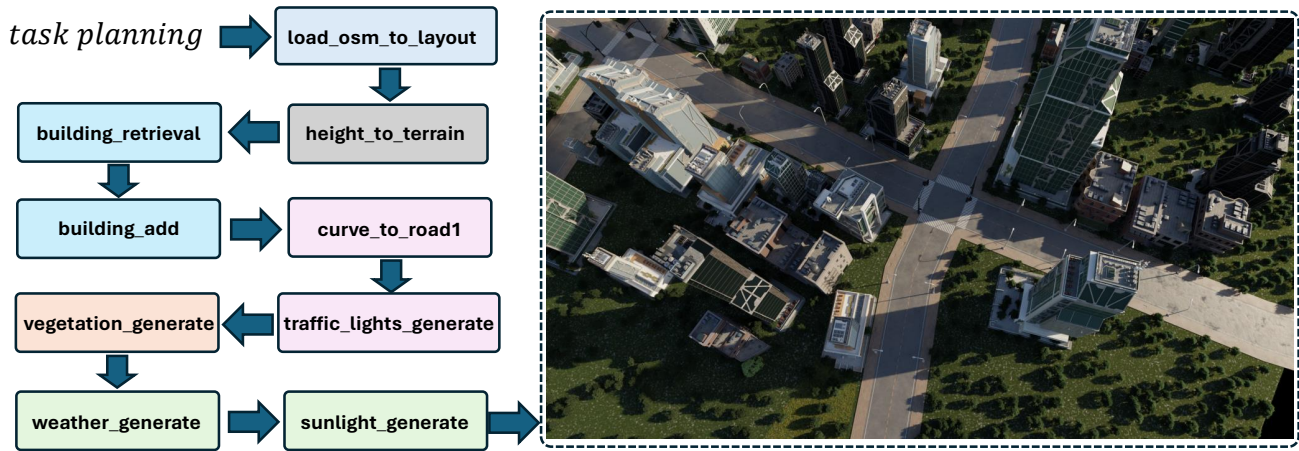


Figure 9. Task phases and PCG module counts in the overall city generation and editing process, with multi-agent system guidance for task selection and execution.

finer specific encapsulation formats. Fig. 11 illustrates several examples of encapsulated PCG modules, where each section’s “Description” also incorporates the mandatory sequential requirements mentioned in Appendix A.1. This ensures that multi-agent systems can plan tasks more accurately by referencing the content within the “Description.”

A.4. Infinite Asset Library and Asset Retrieval

Although many handcrafted assets are exquisite, in urban scene generation tasks, the compatibility between assets and layout is often more important than the complexity of individual assets. To effectively acquire assets that best match



Figure 10. Implementation results of adding dynamic elements.

Table 4. The proportion of API Input/Output Formats and Conversion Interface Statistics. A statistical overview of API input/output formats (in percentages) is presented on the left, where PIDF represents the proportion of input data format types and PODF represents the proportion of output data format types, while the conversion interface along with its descriptions is detailed on the right.

Data Format	PIDF(%)	PODF(%)	Conversion Interface	Description
Scene Layout	0	19.05	Point_to_face_conversion	Converting points to faces.
Noise Function	0.45	0	Cube_generation	Generating cubes.
Image	0.90	0	Point_generation	Generating points.
Texture Material	0.90	32.54	Line_generation	Generating lines.
Geographic Information Data	1.35	0	Face_generation	Generating faces.
Point	3.15	0	Line_to_face_conversion	Converting lines to faces.
Boolean Value	4.50	0	Asset_placement	Placing assets within a scene or environment.
Complex Geometry	4.50	43.65	Point_to_line_conversion	Converting points to lines.
Color	5.86	0	OSM_file_retrieval	Retrieving OpenStreetMap (OSM) files.
Basic Geometry	7.66	0	Object_meshing	Meshing objects.
String Information	8.11	0	Texture_information_extraction	Extracting texture information.
Surface	12.61	2.38	Asset_material_retrieval	Retrieving material data for assets.
Line	13.96	2.38	Asset_mesh_retrieval	Retrieving mesh data for assets.
Random Number	36.04	0	Scene_object_information_extraction	Extracting scene object information.

the scene layout, we propose an infinite asset library approach. This includes static assets that we manually collect and annotate, as well as an ever-expanding asset library driven by PCG, providing each asset with text descriptions and image renderings. To accelerate and improve the accuracy of asset retrieval, we use a pre-trained CLIP model to convert text into image retrieval for assets. Each asset's rendered image is encoded into a standardized 768-dimensional vector, which is then compared with the embedding vector of the input description. So far, we have collected and annotated 16,933 static assets and 18 PCGs for generating buildings. The collection of static assets involves annotating properties such as asset paths, footprint

dimensions (length, width, and area), center coordinates (with $z = 0$), and asset styles for building assets. Similarly, we record these attributes for PCG-generated buildings. Below is an example JSON structure.

```
{
  "buildings": [
    {
      "path": "City\1825\Assets.blend",
      "collection": "Eu_1_building_8",
      "width": 49,
      "length": 38,
      "area": 1862,
      "coordinates": { "x": 158.5, "y": 165 },
      "style": "modern"
    }, ...
  ], ...
  "plants": [...], ...
}
```

During the building generation process, the following steps are executed:

1. Bounding Rectangle Calculation

For each building area A , its minimum bounding rectangle R is computed to obtain the length l and width w :

$$R = \text{minBoundingRectangle}(A),$$

$$l = \text{length}(R), \quad w = \text{width}(R) \quad (10)$$

2. Aspect Ratio Computation

The aspect ratio of the bounding rectangle is calculated


```

class image_to_layout:
    def __init__(self):
        self.classname = "image_to_layout"
        self.description = """Used to map a semantic map into a scene layout in Blender by converting pixels to points in Blender,
                                then transforming boundary points into semantic regions to generate the layout."""
        self.input = """image_name: The filepath of the semantic map file to import.
                                """
        self.limitation = "'image_name' should be a file path pointing to an image file."

    @staticmethod
    def run(image_path):
        # Define colors and corresponding labels
        colors = {
            # (96, 96, 0): "osm_building",
            (170, 39, 0): "osm_building",
            (0, 96, 0): "forest",
            (0, 96, 96): "construction",
            (0, 0, 96): "osm_water",
            (128, 128, 128): "background"
        }
        # Open image
        try:
            image = np.array(Image.open(image_path).convert("RGB"))
        except FileNotFoundError:
            print("Error: Image file not found.")

```

```

class building_add:
    def __init__(self):
        self.classname = "building_add"
        self.description = "Add and place building assets based on the retrieved building assets information."
        self.input = """'json_path': The json file path that records the building assets information."""
        self.limitation = "Before performing this step, please ensure that the 'layout_generate' step has been completed."

    @staticmethod
    def run(json_path: Annotated[str, f"The json file path that records the information"]):
        try:
            i=0
            bpy.data.objects['Cube'].select_set(True)
            bpy.ops.object.delete(use_global=False)
            with open(json_path, 'r', encoding='utf-8') as f:
                data = json.load(f)
                building_obj_names = data.get('building_obj_name_list', [])
                collections = data.get('collections', [])
                used_assets = []

```

```

class getlocation:
    def __init__(self):
        self.classname = "getlocation"
        self.description = "get the position information of the object."
        self.input = "The name of the object for which is needed to know the position information."
        self.limitation = None

    @staticmethod
    def run(selected_obj: Annotated[str, f"get location from selected object"]) -> Annotated[str, "result."]:
        obj = bpy.data.objects.get(selected_obj)
        loc = list(obj.location)
        return f"the location is {loc}"

```

Figure 11. Examples of Encapsulated PCG Modules

as:

$$\text{aspectRatio} = \frac{l}{w} \quad (11)$$

3. Asset Retrieval and Filtering

Algorithm 1 Generate Running Character in Scene

```
1: Input: Path data (path = curve01), dynamic element parameters (crowd_creation, walk_run, style, category, model_quality, random_color)
2: Output: Generated running character placed in Blender scene
3: Let path = curve01.
4: Let crowd_creation = "single".
5: Let walk_run = "run".
6: Let style = "casual".
7: Let category = "run, male_jog02".
8: Let model_quality = "high_poly".
9: Let random_color = True.
10: Create curve object curve01 in Blender.
11: Set path of curve01 as input path data.
12: Parse parameters:
13:   Assign crowd_creation to "single".
14:   Assign walk_run to "run".
15:   Assign style to "casual".
16:   Assign category to "run, male_jog02".
17:   Assign model_quality to "high_poly".
18:   Assign random_color to True.
19: for each point in path (curve01) do
20:   Calculate movement vector  $\mathbf{v}_{move}$  based on path curvature.
21:   Generate character model with specified parameters:
22:     Apply style = "casual".
23:     Apply category = "run, male_jog02".
24:     Apply model_quality = "high_poly".
25:     Assign color randomly if random_color = True.
26:   Place character instance at position  $\mathbf{p}_{char}$  along path curve01.
27:   Set movement action: if walk_run = "run" then
28:     Assign velocity  $\mathbf{v}_{run}$  for running.
29:   else
30:     Assign velocity  $\mathbf{v}_{walk}$  for walking.
31:   end if
32:   Animate character along path based on velocity and movement vector.
33: end for
34: Output: Place generated running character in scene at position  $\mathbf{p}_{char}$ .
35: Return running character instance.
```

Assets \mathcal{S} are retrieved from the asset database by matching their footprints and ensuring that their aspect ratio

falls within a specified threshold ϵ :

$$\mathcal{S} = \{s \mid \text{footprint}(s) \approx \text{footprint}(R), \text{aspectRatio}(s) \in [\text{aspectRatio} \pm \epsilon]\} \quad (12)$$

If assets with an undefined style tag are identified, the CLIP model is employed to filter the asset that best matches the user’s description s_{clip} .

4. Scaling Factor Calculation

For each candidate asset s_i , the scaling factor α is computed as:

$$\alpha_i = \frac{\min(l, w)}{\min(l_i, w_i)} \quad (13)$$

The final target building is determined by selecting the asset with the smallest scaling factor:

$$s_{target} = \arg \min_{s_i \in \mathcal{S}} \alpha_i \quad (14)$$

5. Position Offset and Rotation

After selecting the target asset s_{target} , its position is adjusted based on the asset’s center coordinates (x_{center}, y_{center}) and placed at the appropriate location within the scene. The rotation angle θ of the target asset is determined by the angular offset of the bounding rectangle:

$$\theta = \text{angle}(R) - \text{angle}(s_{target}) \quad (15)$$

Where $\text{angle}(R)$ is the angle of the bounding rectangle, and $\text{angle}(s_{target})$ is the original rotation angle of the target asset. The final rotation transformation for the target asset is:

$$s_{target} = \text{rotate}(s_{target}, \theta) \quad (16)$$

The asset’s position is then adjusted with an offset $\Delta x, \Delta y$:

$$s_{target} = \text{translate}(s_{target}, \Delta x, \Delta y) \quad (17)$$

A.5. Details of Multi-agent

The Annotator(mentioned in Sec 3.3) labels action functions in two steps: first, summarizing existing functions into consistent concepts guided by prompts; second, labeling each function based on these concepts. An action function may receive multiple labels. Once all action functions are processed, the labeled information is stored in the common message pool, enabling other agents to directly access it.

B. Dataset Synthetic

Synthetic data for urban-scale scenes is widely used in many tasks within computer vision, as real-world data collection incurs significant costs, and manual modeling faces similar challenges. Our method City \mathcal{X} generates synthetic

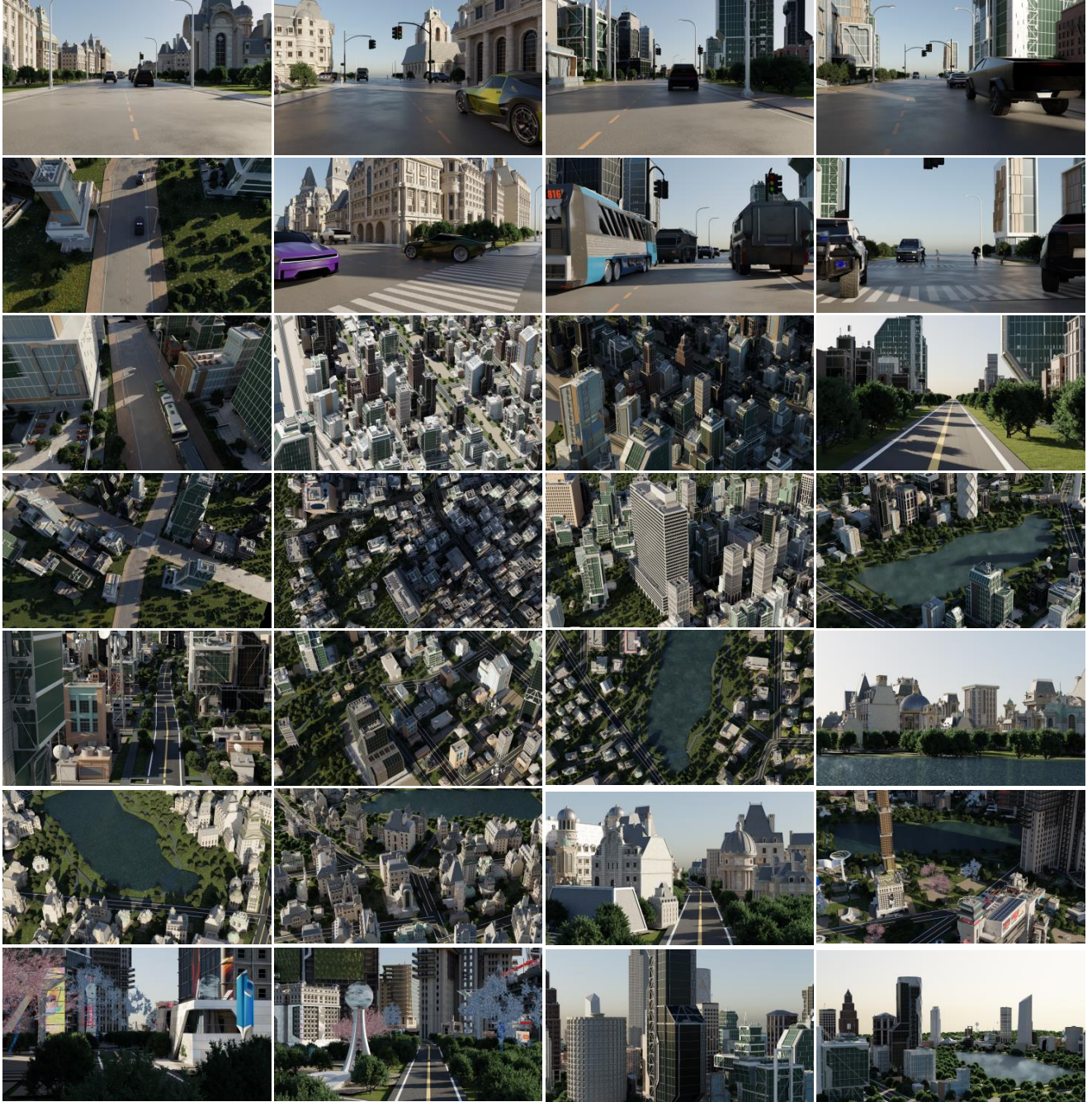


Figure 12. Random Outputs from the Dataset Generator.

datasets with high quality and efficiency while requiring minimal resources. Tab. 5 compares the City \mathcal{X} synthetic dataset with several other urban datasets. We provide a large sample of random RGB images from our dataset generator(Fig. 12), each image was rendered simultaneously for a variety of channels (various specification images for the dataset in Sec 3.4.

C. User Study Details

In our experimental process, we employed manual evaluation to assess the results. An example of the evaluation interface used during this process is shown in Fig. 13. To ensure fairness and objectivity, all evaluation images were anonymized to prevent bias in the assessment. This approach maintained the integrity of the evaluation process,

Table 5. Comparison of CityX Synthetic Dataset with Existing Urban Datasets.

Dataset	Year	Scenes in Total	Assets in Total	Area/Length in Total	Triangles Pre-Scene	Free Assets	Annotation	Provides Code
Semantic3D[16]	2017	3	-	-	4000M	No	Semantic	No
Synscapes[44]	2018	25K	-	-	-	No	Semantic	No
DublinCity[55]	2019	1	-	2km ²	260M	No	Semantic	No
ProcSy[21]	2019	∞	∞	∞	-	Yes	Semantic	No
Campus3D[24]	2020	1	-	1.58km ²	937.1M	No	Hierarchical	No
Meta-Sim2[9]	2020	∞	-	-	-	No	Semantic	No
Hessigheim 3D[22]	2021	1	-	0.19 km ²	125.7M/36.76M	No	Semantic	No
SUM[12]	2021	1	-	4 km ²	19M	No	Semantic	No
STPLS3D[3]	2022	1	-	1.27km ²	150.4M	No	Semantic	No
InstanceBuilding[48]	2022	1	-	0.434km ²	7.46M	No	Semantic	No
UrbanBIS[49]	2023	5	-	10.78km ²	2523.8M/284.3M	No	Semantic/Instance	No
MatrixCity[25]	2024	2	-	28km ²	-	Yes	Semantic/Instance/Depth	Yes
CityX(Ours)	2024	∞	∞	∞	383M/km ²	Yes	Semantic/Instance/Depth	Yes

City Scene Evaluation

City Scene Evaluation: Please rate the following city scene images from the perspectives of visual aesthetics and architectural rationality. The rating scale is as follows: 0-1 represents very poor, 1.0-2.0 represents slightly poor, 2.0-3.0 represents barely acceptable, 3.0-4.0 represents good, and 4.0-5.0 represents excellent.

* 21.



aesthetic score 1 2 3 4 5

rationality score ○ ○ ○ ○ ○

Figure 13. The example questionnaire for participants.

ensuring that each image was judged solely based on its merits.

References

- [1] Tom B. Brown, Benjamin Mann, Nick Ryder, Melanie Subbiah, Jared Kaplan, Prafulla Dhariwal, Arvind Neelakantan, Pranav Shyam, Girish Sastry, Amanda Askell, Sandhini Agarwal, Ariel Herbert-Voss, Gretchen Krueger, Tom Henighan, Rewon Child, Aditya Ramesh, Daniel M. Ziegler, Jeffrey Wu, Clemens Winter, Christopher Hesse, Mark Chen, Eric Sigler, Mateusz Litwin, Scott Gray, Benjamin Chess, Jack Clark, Christopher Berner, Sam McCandlish, Alec Radford, Ilya Sutskever, and Dario Amodei. Language models are few-shot learners, 2020. 8
- [2] Lucy Chai, Richard Tucker, Zhengqi Li, Phillip Isola, and Noah Snavely. Persistent nature: A generative model of unbounded 3d worlds. In *Proceedings of the IEEE/CVF Conference on Computer Vision and Pattern Recognition*, pages 20863–20874, 2023. 3, 7
- [3] Meida Chen, Qingyong Hu, Thomas Hugues, Andrew Feng, Yu Hou, Kyle McCullough, and Lucio Soibelman. Stpls3d: A large-scale synthetic and real aerial photogrammetry 3d point cloud dataset. 15
- [4] Mark Chen, Jerry Tworek, Heewoo Jun, Qiming Yuan, Henrique Ponde de Oliveira Pinto, Jared Kaplan, Harri Edwards, Yuri Burda, Nicholas Joseph, Greg Brockman, et al. Evaluating large language models trained on code. *arXiv preprint arXiv:2107.03374*, 2021. 3
- [5] Mark Chen, Jerry Tworek, Heewoo Jun, Qiming Yuan, Henrique Ponde de Oliveira Pinto, Jared Kaplan, Harri Edwards, Yuri Burda, Nicholas Joseph, Greg Brockman, et al. Evaluating large language models trained on code. *arXiv preprint arXiv:2107.03374*, 2021. 7
- [6] Zhaoxi Chen, Guangcong Wang, and Ziwei Liu. Scenedreamer: Unbounded 3d scene generation from 2d image collections. *arXiv preprint arXiv:2302.01330*, 2023. 3, 7
- [7] Krzysztof Czerwinski. Autogpt. <https://github.com/Significant-Gravitas/AutoGPT>, 2023. v0.5.1. 3
- [8] Jie Deng, Wenhao Chai, Jianshu Guo, Qixuan Huang, Wenhao Hu, Jenq-Neng Hwang, and Gaoang Wang. Citygen: Infinite and controllable 3d city layout generation. *arXiv preprint arXiv:2312.01508*, 2023. 2
- [9] Jeevan Devaranjan, Amlan Kar, and Sanja Fidler. Metasim2: Unsupervised learning of scene structure for synthetic data generation. (arxiv:2008.09092v1 [cs.cv]). *arXiv Computer Science, arXiv Computer Science*, 2020. 15
- [10] Yilun Du, Shuang Li, Antonio Torralba, and Igor Mordatch. Improving factuality and reasoning in language models through multiagent debate. 3
- [11] Patrick Esser, Robin Rombach, and Bjorn Ommer. Taming transformers for high-resolution image synthesis. In *2021 IEEE/CVF Conference on Computer Vision and Pattern Recognition (CVPR)*, 2021. 3
- [12] Weixiao Gao, Liangliang Nan, Bas Boom, and Hugo Ledoux. Sum: A benchmark dataset of semantic urban meshes. *ISPRS Journal of Photogrammetry and Remote Sensing*, page 108–120, 2021. 15
- [13] Cristina Gasch, José Sotoca, Miguel Chover, Inmaculada Remolar, and Cristina Rebollo. Procedural modeling of plant ecosystems maximizing vegetation cover. *Multimedia Tools and Applications*, 81, 2022. 3
- [14] Google DeepMind Gemma Team. Gemma: Open models based on gemini research and technology. See Contributions and Acknowledgments section for full author list. Please send correspondence to gemma-1-report@google.com. 8
- [15] Ran Gong, Qiuyuan Huang, Xiaojian Ma, Hoi Vo, Zane Durante, Yusuke Noda, Zilong Zheng, Song-Chun Zhu, Demetri Terzopoulos, Li Fei-Fei, et al. Mindagent: Emergent gaming interaction. *arXiv preprint arXiv:2309.09971*, 2023. 3
- [16] T. Hackel, N. Savinov, L. Ladicky, J. D. Wegner, K. Schindler, and M. Pollefeys. Semantic3d.net: A new large-scale point cloud classification benchmark. *ISPRS Annals of the Photogrammetry, Remote Sensing and Spatial Information Sciences*, page 91–98, 2017. 15
- [17] Zekun Hao, Arun Mallya, Serge Belongie, and Ming-Yu Liu. Gancraft: Unsupervised 3d neural rendering of minecraft worlds. In *Proceedings of the IEEE/CVF International Conference on Computer Vision*, pages 14072–14082, 2021. 3
- [18] Ziniu Hu, Ahmet Iscen, Aashi Jain, Thomas Kipf, Yisong Yue, David A. Ross, Cordelia Schmid, and Alireza Fathi. Scenecraft: An llm agent for synthesizing 3d scene as blender code, 2024. 2, 4
- [19] Wenlong Huang, Pieter Abbeel, Deepak Pathak, and Igor Mordatch. Language models as zero-shot planners: Extracting actionable knowledge for embodied agents. In *International Conference on Machine Learning*, pages 9118–9147. PMLR, 2022. 3
- [20] Albert Q. Jiang, Alexandre Sablayrolles, Arthur Mensch, Chris Bamford, Devendra Singh Chaplot, Diego de las Casas, Florian Bressand, Gianna Lengyel, Guillaume Lample, Lucile Saulnier, L  lio Renard Lavaud, Marie-Anne Lachaux, Pierre Stock, Teven Le Scao, Thibaut Lavril, Thomas Wang, Timoth  e Lacroix, and William El Sayed. Mistral 7b, 2023. 8
- [21] Samin Khan, Buu Phan, Rick Salay, and Krzysztof Czarnecki. Procsy: Procedural synthetic dataset generation towards influence factor studies of semantic segmentation networks. *Computer Vision and Pattern Recognition, Computer Vision and Pattern Recognition*, 2019. 15
- [22] Michael K  lle, Dominik Laupheimer, Stefan Schmohl, Norbert Haala, Franz Rottensteiner, Jan Dirk Wegner, and Hugo Ledoux. The hessigheim 3d (h3d) benchmark on semantic segmentation of high-resolution 3d point clouds and textured meshes from uav lidar and multi-view-stereo. *ISPRS Open Journal of Photogrammetry and Remote Sensing*, page 100001, 2021. 15
- [23] Hongxin Li, Jingran Su, Yuntao Chen, Qing Li, and Zhaoxiang Zhang. Sheetcopilot: Bringing software productivity to the next level through large language models. *arXiv preprint arXiv:2305.19308*, 2023. 3
- [24] Xinke Li, Chongshou Li, Zekun Tong, Andrew Lim, Junsong Yuan, Yuwei Wu, Jing Tang, and Raymond Huang.

- Campus3d: A photogrammetry point cloud benchmark for hierarchical understanding of outdoor scene. In *Proceedings of the 28th ACM International Conference on Multimedia*, 2020. 15
- [25] Yixuan Li, Lihan Jiang, Linning Xu, Yuanbo Xiangli, Zhenzhi Wang, Dahua Lin, and Bo Dai. Matrixcity: A large-scale city dataset for city-scale neural rendering and beyond. 2023. 15
- [26] Tian Liang, Zhiwei He, Wenxiang Jiao, Xing Wang, Yan Wang, Rui Wang, Yujiu Yang, Zhaopeng Tu, and Shuming Shi. Encouraging divergent thinking in large language models through multi-agent debate. 2023. 3
- [27] Chieh Hubert Lin, Hsin-Ying Lee, Willi Menapace, Menglei Chai, Aliaksandr Siarohin, Ming-Hsuan Yang, and Sergey Tulyakov. Infinitcity: Infinite-scale city synthesis. *arXiv preprint arXiv:2301.09637*, 2023. 2, 3, 7
- [28] Markus Lipp, Daniel Scherzer, Peter Wonka, and Michael Wimmer. Interactive modeling of city layouts using layers of procedural content. In *Computer Graphics Forum*, pages 345–354. Wiley Online Library, 2011. 3
- [29] Arun Mallya, Ting-Chun Wang, Karan Sapra, and Ming-Yu Liu. *World-Consistent Video-to-Video Synthesis*, page 359–378. 2020. 3
- [30] Yohei Nakajima. Babyagi. <https://github.com/yoheinakajima/babyagi>, 2023. 3
- [31] OpenAI. Gpt-4v(ision) system card. System Card, 2023. Version 1.0. 6
- [32] OpenAI, Josh Achiam, Steven Adler, Sandhini Agarwal, Lama Ahmad, Ilge Akkaya, Florencia Leoni Aleman, Diogo Almeida, Janko Altenschmidt, Sam Altman, Shyamal Anadkat, Red Avila, Igor Babuschkin, Suchir Balaji, Valerie Balcom, Paul Baltescu, Haiming Bao, Mohammad Bavarian, Jeff Belgum, Irwan Bello, Jake Berdine, Gabriel Bernadett-Shapiro, Christopher Berner, Lenny Bogdonoff, Oleg Boiko, Madelaine Boyd, Anna-Luisa Brakman, Greg Brockman, Tim Brooks, Miles Brundage, Kevin Button, Trevor Cai, Rosie Campbell, Andrew Cann, Brittany Carey, Chelsea Carlson, Rory Carmichael, Brooke Chan, Che Chang, Fotis Chantzis, Derek Chen, Sully Chen, Ruby Chen, Jason Chen, Mark Chen, Ben Chess, Chester Cho, Casey Chu, Hyung Won Chung, Dave Cummings, Jeremiah Currier, Yunxing Dai, Cory Decareaux, Thomas Degry, Noah Deutsch, Damien Deville, Arka Dhar, David Dohan, Steve Dowling, Sheila Dunning, Adrien Ecoffet, Atty Eleti, Tyna Eloundou, David Farhi, Liam Fedus, Niko Felix, Simón Posada Fishman, Juston Forte, Isabella Fullford, Leo Gao, Elie Georges, Christian Gibson, Vik Goel, Tarun Gogineni, Gabriel Goh, Rapha Gontijo-Lopes, Jonathan Gordon, Morgan Grafstein, Scott Gray, Ryan Greene, Joshua Gross, Shixiang Shane Gu, Yufei Guo, Chris Hallacy, Jesse Han, Jeff Harris, Yuchen He, Mike Heaton, Johannes Heidecke, Chris Hesse, Alan Hickey, Wade Hickey, Peter Hoeschele, Brandon Houghton, Kenny Hsu, Shengli Hu, Xin Hu, Joost Huizinga, Shantanu Jain, Shawn Jain, et al. Gpt-4 technical report, 2023. 8
- [33] Yoav Parish and Pascal Müller. Procedural modeling of cities. pages 301–308, 2001. 3
- [34] Taesung Park, Ming-Yu Liu, Ting-Chun Wang, and Jun-Yan Zhu. Semantic image synthesis with spatially-adaptive normalization. In *2019 IEEE/CVF Conference on Computer Vision and Pattern Recognition (CVPR)*, 2019. 3
- [35] Ken Perlin. An image synthesizer. *ACM SIGGRAPH Computer Graphics*, page 287–296, 1985. 3
- [36] Przemyslaw Prusinkiewicz and Aristid Lindenmayer. *The Algorithmic Beauty of Plants*. 1990. 3
- [37] Alec Radford, JongWook Kim, Chris Hallacy, A. Ramesh, Gabriel Goh, Sandhini Agarwal, Girish Sastry, Askell Amanda, Pamela Mishkin, Jack Clark, Gretchen Krueger, and Ilya Sutskever. Learning transferable visual models from natural language supervision. *Cornell University - arXiv, Cornell University - arXiv*, 2021. 4
- [38] Yongliang Shen, Kaitao Song, Xu Tan, Dongsheng Li, Weiming Lu, and Yueting Zhuang. Hugginggpt: Solving ai tasks with chatgpt and its friends in huggingface. *arXiv preprint arXiv:2303.17580*, 2023. 3, 4
- [39] Chunyi Sun, Junlin Han, Weijian Deng, Xinlong Wang, Zishan Qin, and Stephen Gould. 3d-gpt: Procedural 3d modeling with large language models. *arXiv preprint arXiv:2310.12945*, 2023. 2, 4
- [40] Jerry O Talton, Yu Lou, Steve Lesser, Jared Duke, Radomír Mech, and Vladlen Koltun. Metropolis procedural modeling. *ACM Trans. Graph.*, 30(2):11–1, 2011. 3
- [41] Hugo Touvron, Louis Martin, Kevin Stone, Peter Albert, Amjad Almahairi, Yasmine Babaei, Nikolay Bashlykov, Soumya Batra, Prajjwal Bhargava, Shrutli Bhosale, Dan Bikel, Lukas Blecher, Cristian Canton Ferrer, Moya Chen, Guillem Cucurull, David Esiobu, Jude Fernandes, Jeremy Fu, Wenyin Fu, Brian Fuller, Cynthia Gao, Vedanuj Goswami, Naman Goyal, Anthony Hartshorn, Saghar Hosseini, Rui Hou, Hakan Inan, Marcin Kardas, Viktor Kerkez, Madian Khabsa, Isabel Kloumann, Artem Korenev, Punit Singh Koura, Marie-Anne Lachaux, Thibaut Lavril, Jenya Lee, Diana Liskovitch, Yinghai Lu, Yuning Mao, Xavier Martinet, Todor Mihaylov, Pushkar Mishra, Igor Molybog, Yixin Nie, Andrew Poulton, Jeremy Reizenstein, Rashi Rungta, Kalyan Saladi, Alan Schelten, Ruan Silva, Eric Michael Smith, Ranjan Subramanian, Xiaoqing Ellen Tan, Binh Tang, Ross Taylor, Adina Williams, Jian Xiang Kuan, Puxin Xu, Zheng Yan, Iliyan Zarov, Yuchen Zhang, Angela Fan, Melanie Kambadur, Sharan Narang, Aurelien Rodriguez, Robert Stojnic, Sergey Edunov, and Thomas Scialom. Llama 2: Open foundation and finetuned chat models, 2023. 8
- [42] Carlos Vanegas, Tom Kelly, Basil Weber, Jan Halatsch, Daniel Aliaga, and Pascal Müller. Procedural generation of parcels in urban modeling. *Computer Graphics Forum*, 31: 681–690, 2012. 3
- [43] Guanzhi Wang, Yuqi Xie, Yunfan Jiang, Ajay Mandlekar, Chaowei Xiao, Yuke Zhu, Linxi Fan, and Anima Anandkumar. Voyager: An open-ended embodied agent with large language models. *arXiv preprint arXiv:2305.16291*, 2023. 3
- [44] Magnus Wrenninge and Jonas Unger. Synscapes: A photorealistic synthetic dataset for street scene parsing. *arXiv: Computer Vision and Pattern Recognition, arXiv: Computer Vision and Pattern Recognition*, 2018. 15

- [45] Chenfei Wu, Shengming Yin, Weizhen Qi, Xiaodong Wang, Zecheng Tang, and Nan Duan. Visual chatgpt: Talking, drawing and editing with visual foundation models. *arXiv preprint arXiv:2303.04671*, 2023. 3
- [46] Qingyun Wu, Gagan Bansal, Jieyu Zhang, Yiran Wu, Beibin Li, Erkang Zhu, Li Jiang, Xiaoyun Zhang, Shaokun Zhang, Jiale Liu, AhmedHassan Awadallah, RyenW White, Doug Burger, and Chi Wang. Autogen: Enabling next-gen llm applications via multi-agent conversation. 2023. 3
- [47] Haozhe Xie, Zhaoxi Chen, Fangzhou Hong, and Ziwei Liu. Citydreamer: Compositional generative model of unbounded 3d cities. *arXiv preprint arXiv:2309.00610*, 2023. 2, 7
- [48] Yanghui Xu, Jiazhou Chen, Shufang Lu, Ronghua Liang, and Liangliang Nan. 3d instance segmentation of mvs buildings. 15
- [49] Guoqing Yang, Fuyou Xue, Qi Zhang, Ke Xie, Chi-Wing Fu, and Hui Huang. Urbanbis: a large-scale benchmark for fine-grained urban building instance segmentation. In *Special Interest Group on Computer Graphics and Interactive Techniques Conference Conference Proceedings*, 2023. 15
- [50] Yong-Liang Yang, Jun Wang, Etienne Vouga, and Peter Wonka. Urban pattern: Layout design by hierarchical domain splitting. *ACM Transactions on Graphics (Proceedings of SIGGRAPH Asia 2013)*, 32:Article No. xx, 2013. 3
- [51] Andy Zeng, Maria Attarian, Brian Ichter, Krzysztof Choromanski, Adrian Wong, Stefan Welker, Federico Tombari, Aavek Purohit, Michael Ryoo, Vikas Sindhwani, et al. Socratic models: Composing zero-shot multimodal reasoning with language. *arXiv preprint arXiv:2204.00598*, 2022. 3
- [52] Jian Zhang, Chang-bo Wang, Hong Qin, Yi Chen, and Yan Gao. Procedural modeling of rivers from single image toward natural scene production. *The Visual Computer*, 35, 2019. 3
- [53] Mengqi Zhou, Jun Hou, Shougao Zhang, Chuanchen Luo, Yuxi Wang, Zhaoxiang Zhang, and Junran Peng. Scenex: Procedural controllable large-scale scene generation via large-language models. *arXiv preprint arXiv:2403.15698*, 2024. 2, 4, 7
- [54] Xizhou Zhu, Yuntao Chen, Hao Tian, Chenxin Tao, Weijie Su, Chenyu Yang, Gao Huang, Bin Li, Lewei Lu, Xiaogang Wang, et al. Ghost in the minecraft: Generally capable agents for open-world environments via large language models with text-based knowledge and memory. *arXiv preprint arXiv:2305.17144*, 2023. 3
- [55] S.M.Iman Zolanvari, Susana Ruano, Aakanksha Rana, Alan Cummins, RogérioEduardoda Silva, Morteza Rahbar, and Aljosa Smolic. Dublincity: Annotated lidar point cloud and its applications. *British Machine Vision Conference, British Machine Vision Conference*, 2019. 15